RESEARCH ARTICLE | FEBRUARY 11 2025

Raindrop formation in a thunderstorm mimicking environment under non-uniform electric field

Ming Zhang (张明) ; Zhiwen Yang (杨志文); Chuan Li (李传) ; Jiawei Li (李家玮); Dingchen Li (李丁晨) ; Qixiong Fu (傅琦雄); Kexun Yu (于克训)

Physics of Fluids 37, 022023 (2025)
https://doi.org/10.1063/5.0251043

Physics of Fluids ARTICLE pubs.aip.org/aip/pof

Raindrop formation in a thunderstorm mimicking environment under non-uniform electric field

Cite as: Phys. Fluids **37**, 022023 (2025); doi: 10.1063/5.0251043
Submitted: 29 November 2024 · Accepted: 5 January 2025 ·
Published Online: 11 February 2025

View Online Export Citation CrossMark

Ming Zhang (张明),[1] Zhiwen Yang (杨志文),[1] Chuan Li (李传),[1,a)] Jiawei Li (李家玮),[1] Dingchen Li (李丁晨),[2,a)] Qixiong Fu (傅琦雄),[1] and Kexun Yu (于克训)[1]

AFFILIATIONS

[1]State Key Laboratory of Advanced Electromagnetic Technology, International Joint Research Laboratory of Magnetic Confinement Fusion and Plasma Physics, School of Electrical and Electronic Engineering, Huazhong University of Science and Technology, Wuhan 430074, China

[2]Department of Building Environment and Energy Engineering, The Hong Kong Polytechnic University, Hong Kong 999077, China

[a)]**Authors to whom correspondence should be addressed:** lichuan@hust.edu.cn and 18342212883@163.com

ABSTRACT

The rapid formation of raindrops within thunderstorm clouds is significantly influenced by the synergistic effect of non-uniform electric fields and charge, which facilitates the collision and growth of droplets. This phenomenon forms the theoretical foundation for charged particle catalytic artificial rainfall technology. Despite this, the precise mechanism by which these factors enhance droplet collision and growth remains elusive. In this study, we endeavored to elucidate this mechanism by constructing a non-uniform electric field to emulate the conditions within a lightning environment. We introduced charged–neutral droplet pairs and systematically investigated the impact of electric field gradient and charge on droplet collision characteristics, specifically the likelihood and frequency of collisions, under various reference field strength conditions. Our findings indicate that when the reference field strength is below 1.75×10^5 V · m^{-1}, the decaying gradient electric field and the increase in charge significantly enhances the likelihood of droplet collisions. Conversely, a higher electric field gradient is associated with a decreased collision frequency, while a higher charge has a positive effect on this frequency. These insights not only contribute to a deeper comprehension of the mechanisms by which non-uniform electric fields and charge promote droplet collision and growth within thunderstorm clouds but also offer theoretical underpinnings for the optimization of charged particle catalytic artificial rainfall technology.

I. INTRODUCTION

Artificial rainfall technology has played a great role in alleviating drought, replenishing water resources, and improving the living environment of human beings.[1,2] As an emerging rainfall technology, artificial rainfall catalyzed by charged particles has a low dependence on chemical catalysts compared with traditional artificial rainfall technology. It is based on the synergistic effect of electric field and charge, accelerating the growth of droplet collision to form raindrops[3–5] and is an environmentally friendly artificial rainfall technology.[6]

Gas ionization forms charged particle clusters that create plasmas and has many applications.[7–10] Their interaction with water molecules charges droplets, producing distinct properties. In order to reveal the internal mechanism of electric field and charge promoting droplet collision, predecessors have conducted research from the perspectives of electric field strength,[11] charge level,[12] and droplet size.[13] Beard *et al.*[14] conducted cloud chamber experiments showing that even the smallest charge can significantly increase the coalescence likelihood when two droplets collide. Guo *et al.*[15] found through numerical studies that for clouds with initial droplet sizes less than 10 μm, charge significantly enhances droplet collisions, and the presence of an electric field further accelerates coalescence and the formation of larger droplets. Li *et al.*[11] studied the collision characteristics of two droplets under different uniform electric fields, finding that the improvement effect of the applied electric field force on droplet collisions differs from that of electrostatic force.

Direct observational data on the electric field gradient in thunderstorm clouds remains scarce due to technical challenges and complexities in actual measurements. We referred to electric field distribution near the corona discharge needle electrode, which is the order of 107 V/m^2. This is also introduced in the manuscript. At the begin of this paragraph, we simply pointed out the non-uniformity of the electric field and the high charge characteristics.[16,17] As Sun *et al.*[18] found that electric field forces in thunderstorm clouds can cause local charge density changes of -0.6 to 0.12 nC · m^{-3}, leading to a redistribution of

charge structures and an increase in local vertical electric field strengths by up to 5 $kV \cdot m^{-1}$. Zhou and Tinsley[19] simulated the current density flow in layer clouds, with the atmospheric electric field gradient in the model reaching about 200 $V \cdot m^{-2}$. However, it is not a thunderstorm cloud. Since lightning discharge involves rapid current flow and electrical breakdown of air, the electric field gradient near a lightning channel can be very large. Direct observational data on the electric field gradient in thunderstorm clouds are still relatively scarce. Liu *et al.*[20] studied the electric field distribution near a corona discharge needle electrode, where the electric field gradient can reach the order of 10^7 $V \cdot m^{-2}$, providing a reference for the study of electric field gradients in thunderstorm clouds.

Although previous relevant studies have adopted non-uniformly distributed electric field and charge conditions, for instance, Washizu and Jones[21] investigated the dielectrophoretic force induced by electric field gradient on a single particle in non-uniform electric fields but did not account for the overall impact of multiple dynamic forces on the collision behavior of droplets. Li *et al.*[22,23] found in corona discharge environments generated by wire-mesh or needle-mesh electrodes that the combined effect of electric field and charge can facilitate droplet collection, these studies are mainly macroscopic. Additionally, Li *et al.*[24] used discharge plasma to charge and polarize droplets, creating gradient electric fields and charge distributions in space to control droplet transport. However, this differs from the issue of droplet collisions in clouds. Moreover, in our earlier experiments in a cloud chamber with corona discharge, we observed sub-micron droplets growing into large droplets over 25 μm, primarily attributed to significantly enhanced collision interactions due to the uneven distribution of electric field and charge.[25] However, the intrinsic mechanisms by which this uneven distribution affects droplet collision and coalescence remain unclear. Thus, we conducted further research on the effects of gradient electric fields on droplet collision.

Charged droplets with the same polarity will repel each other when they are at relatively long distances, while charged droplets and neutral droplets will always attract each other regardless of distance.[3] Additionally, in practical environments, strong collisions in the initial stage can quickly deplete the net charge of droplets carrying opposite polarities, diminishing the net effect of charge on the overall collision and growth of droplet population.[26] However, monopolar charges are not neutralized upon collision, maintaining their influence throughout the interaction process. Consequently, neutral droplets are inclined to aggregate in the vicinity of charged droplets. This study, therefore, concentrates on the collisions between charged and neutral droplets, which is also a critical issue in research areas such as artificial rain enhancement and electrostatic fog removal. Additionally, charged droplets in thunderclouds can carry very high charge levels, yet there is currently a lack of research on the internal interaction mechanisms between highly charged droplets and neutral droplets during collisions.

In summary, previous studies have lacked research on the effects of high charge level and electric field non-uniformity, particularly gradient fields, on the internal mechanisms of collisions between charged and neutral cloud droplets. Therefore, this study focuses on the collision characteristics of a charged–neutral droplet pair under varying reference field strengths and gradient sizes, with both the electric field and gradient directed vertically downward. A trajectory model is employed to calculate the collision efficiency and kernel to characterize the collision properties.

II. MODELS AND METHODOLOGY

In this study, we examine the gravity $\boldsymbol{F}_G$, dielectrophoretic force $\boldsymbol{F}_{DEF}$, mirror electric field force $\boldsymbol{F}_{EF}$, applied electric field force $\boldsymbol{F}_{AE}$, and drag force $\boldsymbol{F}_D$ acting on droplets in uniform and gradient electric fields, as illustrated in Fig. 1. The specific expressions of each force are as follows.

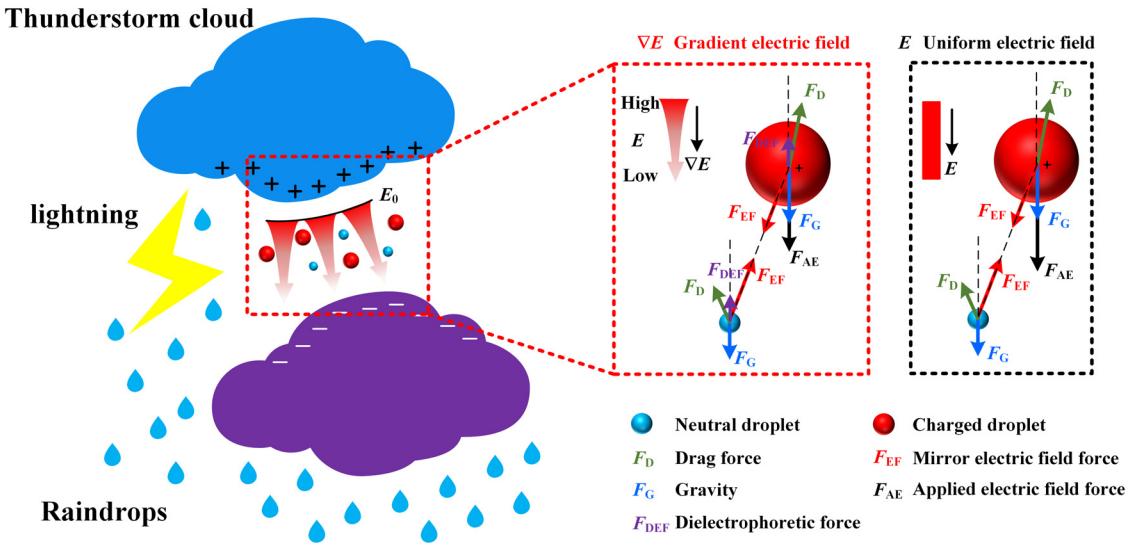

FIG. 1. Force diagram of a charged–neutral droplet pair under gradient electric field and uniform electric field. The electric field $\boldsymbol{E}$ and electric field gradient $\nabla\boldsymbol{E}$ are vertically downward, and the gradient is negative, that is, the electric field decays downward. Note that the mirror electric field force $\boldsymbol{F}_{EF}$ and the applied electric field force $\boldsymbol{F}_{AE}$ can be combined into electrostatic force $\boldsymbol{F}_e$.

The gravity $\boldsymbol{F}_{\mathbf{G}}$ on the droplet is defined as

$$\boldsymbol{F}_{\mathbf{G}} = \frac{4}{3}\pi\rho_{water} r^3 \mathbf{g}, \tag{1}$$

where ρ_{water} is the density of water, r is the radius of the droplet, and $\mathbf{g}$ is the gravitational acceleration.

Due to their inherent polarity, droplets exhibit polarization under an external electric field, forming an induced dipole moment that interacts with the non-uniform electric field, generating dielectrophoretic force.[27] Its expression is as follows:[21]

$$\boldsymbol{F}_{\mathbf{DEF}} = 2\pi r^3 \varepsilon_0 \nabla E^2 \left(\frac{\varepsilon_1 - \varepsilon_0}{\varepsilon_1 + 2\varepsilon_0}\right), \tag{2}$$

where ε_0 and ε_1 are the permittivity of air and water, respectively. E is the electric field strength.

The mirror electric field force $\boldsymbol{F}_{\mathbf{EF}}$ and the applied electric field force $\boldsymbol{F}_{\mathbf{AE}}$ are integrated into the unified calculation of electrostatic force $\boldsymbol{F}_{\mathbf{e}}$, using Davis's high-precision electrostatic force calculation formula,[28,29] as follows:

$$\begin{cases} F_{e1x} = E\cos\delta(q_1 + q_2) - F_{e2x}, \\ F_{e1y} = E\sin\delta(q_1 + q_2) - F_{e2y}, \\ F_{e2x} = Eq_2\cos\delta + \{4\pi\varepsilon_0 r_2^2 E^2 (F_1\cos^2\delta + F_2\sin^2\delta) \\ \qquad + E\cos\delta(F_3 q_1 + F_4 q_2) \\ \qquad + (F_5 q_1^2 + F_6 q_1 q_2 + F_7 q_2^2)/(4\pi\varepsilon_0 r_2^2)\}, \\ F_{e2y} = Eq_2\sin\delta + \{4\pi\varepsilon_0 r_2^2 E^2 F_8 \sin 2\delta \\ \qquad + E\sin\delta(F_9 q_1 + F_{10} q_2)\}, \end{cases} \tag{3}$$

where δ is the angle between the electric field and the line connecting the centers of the two droplets. ε_0 is the permittivity of air. q_1 and q_2 denote the charges, while r_1 and r_2 represent the radii of the two droplets, respectively. F_1–F_{10} are a series of complex dimensionless coefficients.

The drag force $\boldsymbol{F}_{\mathbf{D}}$ acting on a droplet in air is[11]

$$\boldsymbol{F}_{\mathbf{D}} = -\frac{C_D}{2C} A\rho_{air} |\boldsymbol{V} - \boldsymbol{u}|(\boldsymbol{V} - \boldsymbol{u}), \tag{4}$$

where C_{D} and C are the drag coefficient and the Cunningham correction coefficient, respectively. A is the maximum cross-sectional area of the droplet, ρ_{air} is the air density, $\boldsymbol{V}$ and $\boldsymbol{u}$ denote the velocity of the droplet and the disturbance velocity (the flow velocity field induced by the droplet), respectively.

The hydrodynamic interaction between the two droplets is explained using the superposition method,[30] assuming that one droplet moves within the disturbance flow field generated by the other droplet. The calculation of disturbance velocity $\boldsymbol{u}$ is based on the improved superposition method.[31]

Droplet collision characteristics are characterized by collision efficiency η and collision kernel K, which, respectively, represent the likelihood and frequency of droplet collision. Specifically, they can be expressed as follows:[15,32]

$$\eta = \frac{d_{\max}^2}{(r_1 + r_2)^2}, \tag{5}$$

$$K = \eta\pi(r_1 + r_2)^2 |\boldsymbol{V}_1 - \boldsymbol{V}_2|, \tag{6}$$

where $d_{\max}$ is the maximum horizontal distance at which two droplets can collide and r is the radius of the droplet. $\boldsymbol{V}$ is the terminal velocity of the droplet, which represents the steady-state velocity of the droplet relative to the fluid in the absence of any other droplets.

As the reference field strength E_0 increases, the magnitude of electric field gradient $|\nabla \boldsymbol{E}|$ needs to increase a corresponding order of magnitude before there is a significant change in collision efficiency or kernel. To provide a unified representation, we introduce the ratio of electric field gradient *REG*, which represents the ratio of the magnitude of electric field gradient to the value of reference field strength,

$$REG = \frac{|\nabla \boldsymbol{E}|}{E_0}, \tag{7}$$

where $|\nabla \boldsymbol{E}|$ and E_0 represent the magnitude of electric field gradient and reference field strength, respectively. *REG* has units of m^{-1}.

The reference field strength E_0 refers to the maximum value of electric field in the local space where the droplet moves relatively. In our study, the electric field decays downward, and E_0 refers to the electric field strength at the position where the electric field begins to decay in the chosen research space. E_0 is closely related to the average electric field strength in the local space surrounding the droplet's motion.

In clear weather, the electric field strength is approximately 10^2 $\text{V}\cdot\text{m}^{-1}$, while thunderstorm electrification can increase the field to several hundred kilovolts per meter.[33] In this study, the reference field strength E_0 ranges from 10^3 to 10^6 $\text{V}\cdot\text{m}^{-1}$, with varying gradient changes in the vertical direction. This serves as a simulation of droplet collision and coalescence in the uneven electric field environment found in localized regions of thunderstorm clouds. In this study, to clarify the influence of electric field gradient, we calculate using a fixed size of droplet pairs. The radii of charged and neutral droplets are $r_1 = 10\,\mu\text{m}$ and $r_2 = 1\,\mu\text{m}$, respectively. The charge of the charged droplet is $q = (0\text{–}1)\ Q_{\text{Ray}} = (0\text{–}1) \times 8\pi(\varepsilon_0\sigma_0 r^3)^{1/2}$, where Q_{Ray} is the Rayleigh limit charge at which the droplet is on the verge of breaking up due to repulsion between charges.[34,35] ε_0 is the permittivity of air and σ_0 is the surface tension of water.

In the computational model, we employ the second-order Runge–Kutta method[36] to solve the equations of motion for the droplets. The initial disturbance velocities of the two droplets as well as the mirror electric field forces are set to zero.

III. RESULTS AND DISCUSSION

To characterize the likelihood of droplet collisions across varying electric fields, we calculated the collision efficiency. Figure 2 shows the effects of ratio of electric field gradient *REG* on the collision efficiency of a charged–neutral droplet pair under different reference field strengths E_0, with droplet radius and charge held constant. As illustrated in Fig. 2, when the reference field strength $E_0 = 10^3$, 10^4, and 10^5 $\text{V}\cdot\text{m}^{-1}$, the collision efficiency in the gradient electric field is greater than that in the uniform electric field (that is when $REG = 0$). Furthermore, as the magnitude of the electric field gradient $|\nabla \boldsymbol{E}|$ increases, which corresponds to an increase in *REG* in the figure, the collision efficiency improves. For instance, when the reference field strength $E_0 = 10^4$ $\text{V}\cdot\text{m}^{-1}$, the collision efficiency can be nearly doubled at its maximum. Comparatively, the improvement in collision efficiency is more conspicuous at a relatively higher reference field strength. However, when the reference field strength $E_0 = 10^6$ $\text{V}\cdot\text{m}^{-1}$, the collision efficiency in the gradient electric field is lower than that in

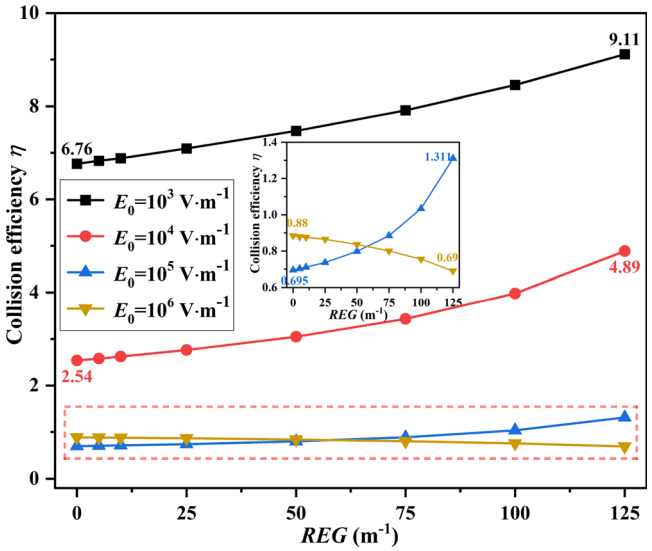

FIG. 2. Effects of ratio of electric field gradient *REG* on the collision efficiency of a charged–neutral droplet pair, with a set of reference field strengths E_0 varying from 10^3 to 10^6 V · m^{-1}. $REG = |\nabla \boldsymbol{E}|/E_0$ is the ratio of magnitude of the electric field gradient to the value of reference field strength. The radii of the charged and neutral droplets are $r_1 = 10\ \mu$m and $r_2 = 1\ \mu$m, respectively. The charge of the charged droplet is 0.1 times the Rayleigh limit charge.

the uniform electric field, as shown in the enlarged section of Fig. 2. Furthermore, as the electric field gradient magnitude $|\nabla \boldsymbol{E}|$ increases, which corresponds to an increase in *REG* in the figure, the collision efficiency decreases. However, the reduction of collision efficiency is relatively minor.

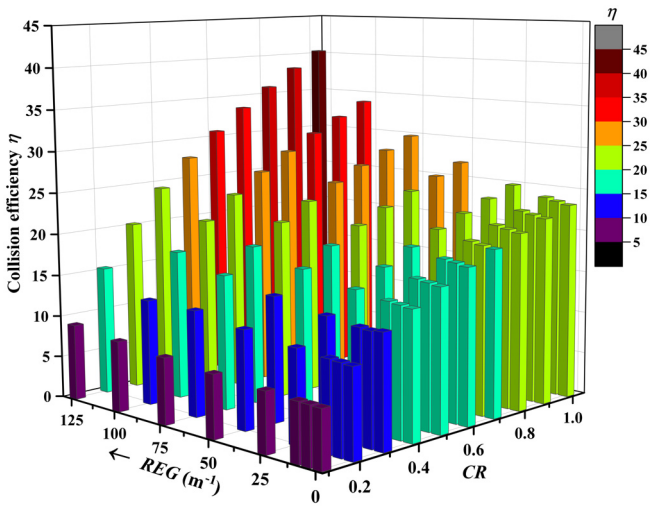

FIG. 3. Effects of ratio of electric field gradient *REG* and charge ratio CR on the collision efficiency of a charged–neutral droplet pair, with reference field strength $E_0 = 10^3$ V · m^{-1}. The radii of the charged and neutral droplets are $r_1 = 10\ \mu$m and $r_2 = 1\ \mu$m, respectively. $CR = Q/Q_{Ray}$ is the ratio of the charged droplet's actual charge to the Rayleigh limit charge.

In addition, as shown in Fig. 3, the effects of the ratio of electric field gradient *REG* and the charge ratio *CR* on the collision efficiency of the droplet pair were further investigated under a reference field strength value of $E_0 = 10^3$ V · m^{-1}. It can be observed that, under the same magnitude of electric field gradient, an increase in charge ratio *CR*, that is, the amount of charge on the charged droplet, significantly improves the collision efficiency. Furthermore, as the electric field gradient magnitude $|\nabla \boldsymbol{E}|$ increases (corresponding to the increase in *REG* in the figure), the collision efficiency improves under each charge ratio *CR*. The improvement is even more pronounced at higher charge ratios.

In summary, it indicates that the gradient electric field facilitates an increased likelihood of collisions when the reference field strength $E_0 = 10^3$, 10^4, and 10^5 V · m^{-1}. The enhancement in collision efficiency is more pronounced when the charged droplets have higher charges and the electric field gradients are larger. In contrast, the gradient electric field instead diminishes the likelihood of collisions when the reference field strength $E_0 = 10^6$ V · m^{-1}.

To find out the internal reasons for the above changes in collision efficiency, we investigated the relationship between the collision efficiency of a charged–neutral droplet pair and the strength of the uniform electric field. As shown in Fig. 4, the collision efficiency decreases as the electric field E increases when E is less than 1.75×10^5 V · m^{-1}. When E is greater than 1.75×10^5 V · m^{-1} and less than 10^7 V · m^{-1}, the collision efficiency increases slightly with increase in E, and finally tends to about 1.0, which is similar to the change rule in the study of Li.[11]

Since we apply a negative electric field gradient, that is, the electric field decays vertically, the variation of collision efficiency in Fig. 2 is largely influenced by the attenuation of electric field. In Fig. 2, when the electric field is below 10^5 V · m^{-1}, the collision efficiency increases with the rising ratio of electric field gradient *REG*. When E exceeds 10^5

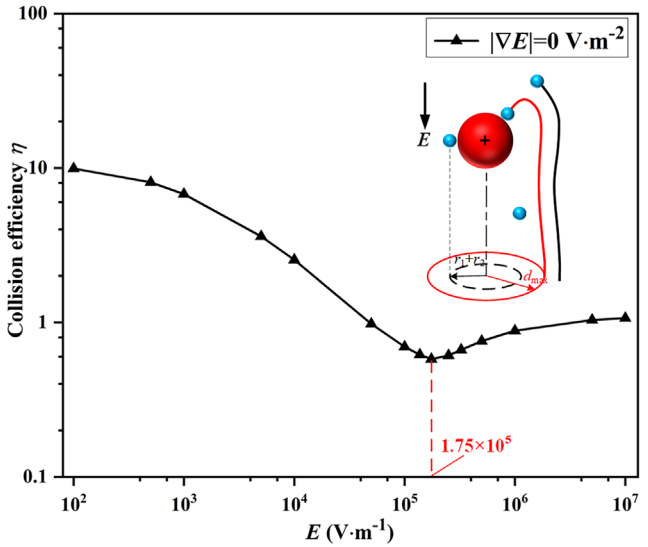

FIG. 4. Effects of the strength of uniform electric field E on the collision efficiency. The electric field gradient is $|\nabla \boldsymbol{E}| = 0$ V · m^{-2}. The radii of the charged and neutral droplets are $r_1 = 10\ \mu$m and $r_2 = 1\ \mu$m, respectively. The charge of the charged droplet is 0.1 times the Rayleigh limit charge.

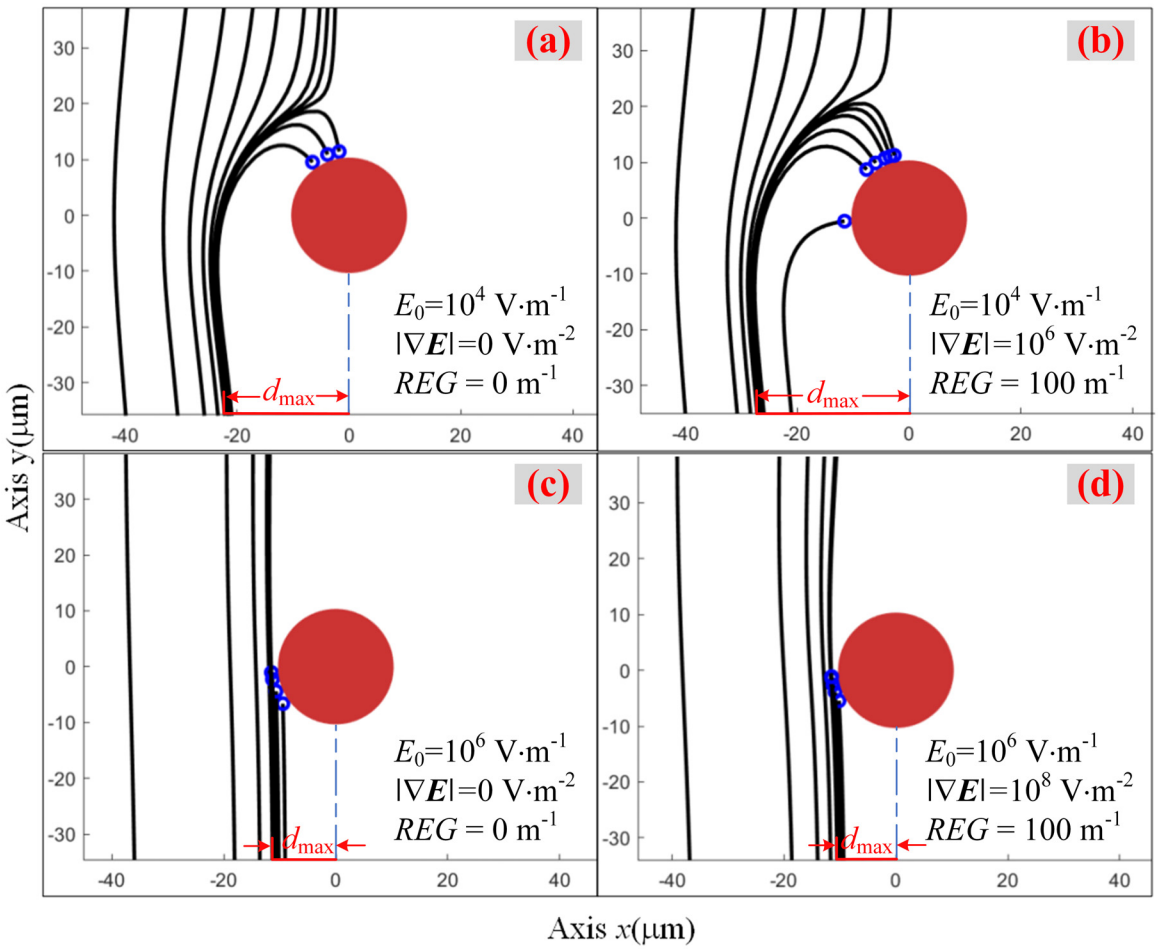

FIG. 5. Relative motion trajectories of a charged droplet (solid red circle) and a neutral droplet (blue circle) under uniform and gradient electric fields. Reference field strength values: (a), (b) $E_0 = 10^4\ \mathrm{V \cdot m^{-1}}$; (c), (d) $E_0 = 10^6\ \mathrm{V \cdot m^{-1}}$. Electric field gradient magnitudes: (a), (d) $|\nabla \boldsymbol{E}| = 0\ \mathrm{V \cdot m^{-2}}$; (b) $|\nabla \boldsymbol{E}| = 10^6\ \mathrm{V \cdot m^{-2}}$; (d) $|\nabla \boldsymbol{E}| = 10^8\ \mathrm{V \cdot m^{-2}}$. $REG = |\nabla \boldsymbol{E}|/E_0$ is the ratio of magnitude of the electric field gradient to the value of reference field strength. The charge of the charged droplet is 0.1 times the Rayleigh limit charge.

$\mathrm{V \cdot m^{-1}}$, the collision efficiency slightly decreases as the ratio of electric field gradient *REG* increases.

Figure 5 further explores the relative motion trajectories of a charged–neutral droplet pair under uniform and gradient vertical downward electric fields. At low reference field strengths, the maximum horizontal distance d_{max} for collisions between the charged–neutral droplet pair in the gradient electric field [Fig. 5(b)] is greater than in the uniform electric field [Fig. 5(a)]. At high reference field strengths, d_{max} in the gradient field [Fig. 5(d)] is slightly less than in the uniform field [Fig. 5(c)]. Combined with the research of Li *et al.*,[11] the internal factors affecting collision efficiency due to the electric field gradient are as follows.

When $E < 1.75 \times 10^5\ \mathrm{V \cdot m^{-1}}$, collisions are primarily driven by electrostatic attraction. However, as the electric field strength increases, the acceleration of charged droplets intensifies, causing greater disturbances that reduce collision likelihood. In a gradient electric field, the vertical component weakens, reducing the acceleration and disturbances on the droplets, thus improving the collision efficiency. Additionally, the gradient field enhances the polarization effect between droplets,[27] increasing their electrostatic attraction and promoting collisions. As the electric field strengthens further, the inertial effect becomes more pronounced and offsets the influence of disturbance to a certain extent.[11] Consequently, the collision efficiency under the uniform electric field experiences a modest enhancement. However, in the gradient electric field with a relatively high reference field strength, the increasing gradient will weaken the inertial effect, resulting in a slight decrease in collision efficiency.

On the other hand, we calculate the collision kernel to quantify the frequency of droplet collisions across varying electric fields. Figure 6 shows the effects of the ratio of electric field gradient *REG*, which is essentially the magnitude of the electric field gradient $|\nabla \boldsymbol{E}|$, on the collision kernel of a charged–neutral droplet pair under different reference field strengths. It can be seen that for reference field strength E_0 ranging from 10^3 to $10^5\ \mathrm{V \cdot m^{-1}}$, the collision kernel under the gradient electric field ($REG > 0$) in the same reference field strength is slightly lower than those under the uniform electric field ($REG = 0$).

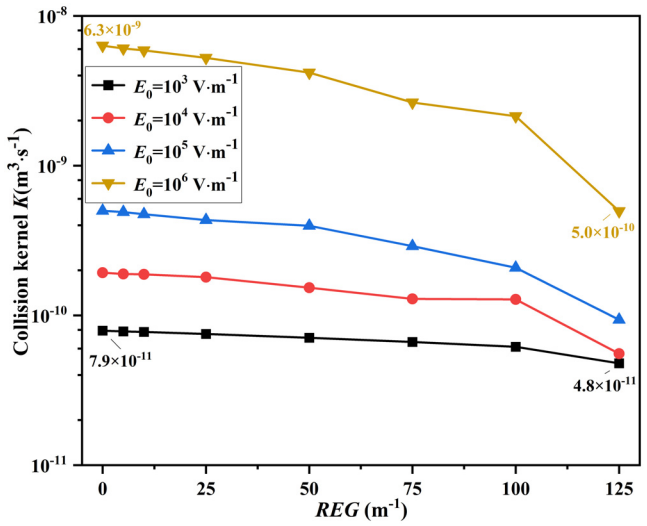

FIG. 6. Effects of ratio of electric field gradient *REG* on the collision kernel of a charged–neutral droplet pair, with a set of reference field strengths E_0 varying from 10^3 to 10^6 V · m^{-1}. $REG = |\nabla \boldsymbol{E}|/E_0$ is the ratio of magnitude of the electric field gradient to the value of reference field strength. The radii of the charged and neutral droplets are $r_1 = 10\ \mu$m and $r_2 = 1\ \mu$m, respectively. The charge of the charged droplet is 0.1 times the Rayleigh limit charge.

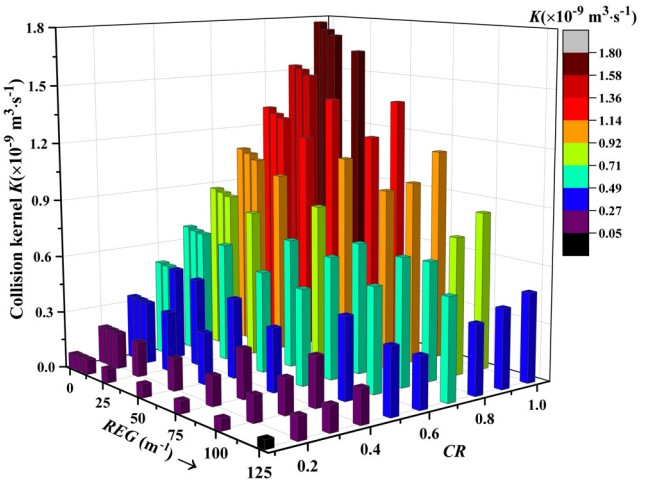

FIG. 7. Effects of ratio of electric field gradient *REG* and charge ratio *CR* on the collision kernel of a charged–neutral droplet pair, with reference field strength $E_0 = 10^3$ V · m^{-1}. The radii of the charged and neutral droplets are $r_1 = 10\ \mu$m and $r_2 = 1\ \mu$m, respectively. $CR = Q/Q_{\text{Ray}}$ is the ratio of the charged droplet's actual charge to the Rayleigh limit charge.

Moreover, as the magnitude of electric field gradient $|\nabla \boldsymbol{E}|$ increases, corresponding to the increase in *REG* shown in the figure, the collision kernel decreases. This trend is more pronounced for a reference field strength of 10^6 V · m^{-1}. In addition, when the reference field strength E_0 is larger, the corresponding collision kernel under the same *REG* is also larger, that is, the collision frequency is higher.

Since the collision frequency is closely related to the droplet's velocity, as shown in the collision kernel calculation formula in Eq. (6), the background electric field in the gradient electric field is attenuated compared to the uniform electric field. That is, the overall average electric field strength in the space where droplets move is lower and will further decrease as the *REG* increases (electric field gradient $|\nabla \boldsymbol{E}|$ increases). This in turn leads to a decrease in the acceleration of the charged droplet in the gradient electric field, while the movement speed of the neutral droplet is not significantly affected. Eventually, the speed difference between two droplets $|\boldsymbol{V}_1 - \boldsymbol{V}_2|$ significantly decreases, and the frequency of droplet collisions per unit time also decreases. Therefore, for the same reference field strength E_0, the collision kernel in the gradient electric field ($REG > 0$) will be lower than that in the uniform electric field ($REG = 0$) and will further decrease as the *REG* increases (electric field gradient $|\nabla \boldsymbol{E}|$ increases). In addition, for the same *REG*, when the reference field strength E_0 is larger, the overall average electric field in the droplet movement space also increases. This can make the accelerated motion of the charged droplets in the electric field more significant, which is conducive to the improvement of the droplet collision frequency, that is, a larger collision kernel.

In addition, Fig. 7 shows the effects of the ratio of electric field gradient *REG* and the charge ratio *CR* on the collision kernel of the droplet pair, investigated under a reference field strength of $E_0 = 10^3$ V · m^{-1}. It can be observed that, for the same charge ratio *CR*, when the electric field gradient magnitude $|\nabla \boldsymbol{E}|$ is larger (corresponding to larger *REG* values in the figure), the collision kernel decreases. However, under the same electric field gradient (corresponding to the same *REG*), an increase in the charge ratio *CR* significantly enhances the collision kernel, which means the collision frequency increases. Therefore, although the gradient electric field in thunderclouds is not beneficial for the frequency of droplet collisions, the large number of charged particles in the thundercloud can increase the charge on droplets, significantly improving this situation and enhancing the collision kernel.

As mentioned earlier, the collision kernel characterizes the frequency of droplet collisions, and it is closely related to the droplets' velocity. The underlying reason for the effect of *REG* on the collision kernel at the same charge ratio *CR* is the same as described in Fig. 6. Specifically, the overall average electric field strength in the background space corresponding to the gradient electric field is lower, which results in a decrease in acceleration of the charged droplet in the gradient electric field. Consequently, the frequency of droplet collisions per unit time is lower, meaning the collision kernel is smaller. On the other hand, when the droplet charge ratio *CR* increases, meaning the charge on the droplets increases, the applied electric field force and the mirror electric field force on the droplets increase significantly, which in turn causes the droplets' acceleration in the background electric field to become more significant. Ultimately, the collision frequency per unit time increases, that is, the collision kernel increases.

IV. CONCLUSIONS

In this paper, we utilize a trajectory model and introduce the ratio of electric field gradient *REG* to examine the collision characteristics of charged–neutral droplet pairs under diverse reference field strengths, magnitudes of electric field gradient, and amounts of charge. The collision characteristics are delineated by two key metrics: collision efficiency and collision kernel, which respectively indicate the likelihood

and frequency of droplet collisions. The findings are presented as follows:

Regarding collision efficiency, when the reference field strength E_0 is less than $1.75 \times 10^5\ \mathrm{V \cdot m^{-1}}$, the weakened gradient electric field and the increase in charge are conducive to increasing the likelihood of collision. Conversely, when the reference field strength E_0 is greater than $1.75 \times 10^5\ \mathrm{V \cdot m^{-1}}$, the gradient electric field instead diminishes the likelihood of collisions, though the degree of reduction is relatively minor. Additionally, the gradient electric field somewhat diminishes the frequency of collisions under different reference field strengths. However, a higher charge amount can effectively enhance the collision frequency. That is, the large number of charged particles in thunderclouds can increase the charge on droplets, thereby significantly mitigating the reduction in collision frequency caused by electric field decay and enhancing the collision kernel.

It is expected that droplet groups have more obvious velocity differences in the gradient electric field, and there may be more obvious collision effects. Future studies could consider the effect of electric field heterogeneity on the evolution of droplet size distribution.

ACKNOWLEDGMENTS

This work is supported by the National Natural Science Foundation of China (Grant No. 52207158).

AUTHOR DECLARATIONS

Conflict of Interest

The authors have no conflicts to disclose.

Author Contributions

Chuan Li and Dingchen Li contributed equally to this paper.

Ming Zhang: Conceptualization (equal); Investigation (equal); Methodology (equal); Writing – review & editing (equal). **Zhiwen Yang:** Conceptualization (equal); Formal analysis (equal); Methodology (equal); Validation (equal); Writing – original draft (equal). **Chuan Li:** Conceptualization (equal); Funding acquisition (equal); Writing – review & editing (equal). **Jiawei Li:** Conceptualization (equal); Formal analysis (equal); Investigation (supporting). **Dingchen Li:** Conceptualization (supporting); Writing – review & editing (equal). **Qixiong Fu:** Conceptualization (supporting). **Kexun Yu:** Conceptualization (supporting).

DATA AVAILABILITY

The data that support the findings of this study are available from the corresponding author upon reasonable request.

REFERENCES

[1]W. Zheng, H. Ma, M. Zhang, F. Xue, K. Yu, Y. Yang, S. Ma, C. Wang, Y. Pan, Z. Shu, J. Mu, W. Yang, and X. Yin, "Evaluation of the first negative ion-based cloud seeding and rain enhancement trial in China," Water **13**, 2473 (2021).
[2]Y. Yang, H. Chen, C. Li, and P. Wang, "Ion induced nucleation of charged droplets enhanced by external electric field," Phys. Plasmas **31**, 73505 (2024).
[3]B. A. Tinsley, R. P. Rohrbaugh, M. Hei, and K. V. Beard, "Effects of image charges on the scavenging of aerosol particles by cloud droplets and on droplet charging and possible ice nucleation processes," J. Atmos. Sci. **57**, 2118–2134 (2000).
[4]S. H. Lee, J. M. Reeves, J. C. Wilson, D. E. Hunton, A. A. Viggiano, T. M. Miller, J. O. Ballenthin, and L. R. Lait, "Particle formation by ion nucleation in the upper troposphere and lower stratosphere," Science **301**, 1886–1889 (2003).
[5]Y. Yang, S. Yang, and C. Li, "Insulator defect detection under extreme weather based on synthetic weather algorithm and improved YOLOv7," High Voltage 1–9 (2024).
[6]R. G. Harrison, G. J. Marlton, M. H. P. Ambaum, and K. A. Nicoll, "Modifying natural droplet systems by charge injection," Phys. Rev. Res. **4**, L022050 (2022).
[7]W. Tong, H. Li, D. Liu, Y. Wu, M. Xu, and K. Wang, "Study on the changes in the reverse recovery characteristics of high-power thyristor under 14.1 MeV fusion neutron irradiation," Fusion Eng. Des. **211**, 114744 (2025).
[8]A. Jaworek, A. M. Ganan-Calvo, and Z. Machala, "Low temperature plasmas and electrosprays," J. Phys. D: Appl. Phys. **52**, 233001 (2019).
[9]P. Zhang, Y. Guo, J. Wei, F. Yan, C. Ye, X. Lu, P. Jiang, and Y. Cheng, "On the microstructure evolution and fracture behavior of titanium alloy plates subjected to underwater explosion," J. Mater. Res. Technol. **34**, 946–958 (2025).
[10]Y. Yang, Y. Lu, C. Li, H. Chen, S. Yang, and R. Wu, "Study on the formation mechanism of soil discharge dark space under negative dc voltage," IEEE Trans. Plasma Sci. 1–7 (2025).
[11]J. Li, C. Li, P. Wang, F. He, M. Xiao, M. Zhang, Y. Yang, K. Yu, and Y. Pan, "Numerical analysis of collision characteristics between charged drop and neutral droplet under uniform electric field," J. Phys. D: Appl. Phys. **54**, 455201 (2021).
[12]M. Zhang, Z. Yang, C. Li, J. Li, D. Li, Q. Fu, and K. Yu, "Collision characteristics of neutral and highly charged droplets in uniform electric fields," Phys. Fluids **37**, 12005 (2025).
[13]L. Zhang, B. A. Tinsley, and L. Zhou, "Parameterization of in-cloud aerosol scavenging due to atmospheric ionization: Part 3. Effects of varying droplet radius," J. Geophys. Res. Atmos. **123**, 10546–10567, https://doi.org/10.1029/2018JD028840 (2018).
[14]K. V. Beard, I. D. Russell, and H. T. Ochs III, "Coalescence efficiency measurements for minimally charged cloud drops," J. Atmos. Sci. **59**, 233–243 (2002).
[15]S. Guo and H. Xue, "The enhancement of droplet collision by electric charges and atmospheric electric fields," Atmos. Chem. Phys. **21**, 69–85 (2021).
[16]H. Yu, T. Zhang, Y. Chen, W. Lü, X. Zhao, and J. Chen, "Vertical electrical field during decay stage of local thunderstorm near coastline in tropical island," Acta Phys. Sin. **70**, 109201 (2021).
[17]A. Sun, M. Yan, Y. Zhang, and X. Qie, "A numerical study of space charge formation beneath thunderstorm," Chinese Journal of Atmos. Sci. **25**, 16–24 (2001).
[18]L. Sun, X. Qie, E. R. Mansell, Z. Chen, Y. Xu, R. Jiang, and Z. Sun, "Feedback effect of electric field force on electrification and charge structure in thunderstorm," Acta Phys. Sin. **67**, 371–383 (2018).
[19]L. Zhou and B. A. Tinsley, "Production of space charge at the boundaries of layer clouds," J. Geophys. Res. Atmos. **112**, D11203, https://doi.org/10.1029/2006JD007998 (2007).
[20]Z. Liu, P. Wang, C. Li, D. Li, Z. Wang, M. Zhang, Y. Yang, and K. Yu, "Combined effect of charges and external electric field on collision-coalescence of microns and nanoscale droplets: A numerical simulation perspective," J. Mol. Liq. **328**, 115376 (2021).
[21]M. Washizu and T. B. Jones, "Multipolar dielectrophoretic force calculation," J. Electrostat. **33**, 187–198 (1994).
[22]D. Li, C. Li, M. Xiao, J. Li, Z. Yang, Q. Fu, M. Zhang, K. Yu, and Y. Pan, "Deconstructing plasma fog collection technology: An experimental study on factors impacting collection efficiency," J. Phys. D: Appl. Phys. **57**, 75201 (2024).
[23]D. Li, C. Li, M. Zhang, M. Xiao, J. Li, Z. Yang, Q. Fu, P. Wang, K. Yu, and Y. Pan, "Advanced fog harvesting method by coupling plasma and micro/nano materials," ACS Appl. Mater. Interfaces **16**, 10984–10995 (2024).
[24]D. Li, C. Li, T. Liang, J. Li, Z. Yang, Q. Fu, M. Zhang, Y. Yang, K. Yu, Y. Du, and X. Zhao, "Controllable droplet velocity: Exploration of droplet transport based on discharge plasma," Phys. Fluids **36**, 122020 (2024).

[25]P. Wang, C. Li, M. Zhang, J. Li, Z. Liu, Y. Yang, K. Yu, and Y. Pan, "Synergistic effect of charges and electric field: Water droplet condensation and coalescence in a sub-saturated cloud chamber," Plasma Sources Sci. Technol. **29**, 45005 (2020).
[26]A. Khain, V. Arkhipov, M. Pinsky, Y. Feldman, and Y. Ryabov, "Rain enhancement and fog elimination by seeding with charged droplets. Part I: Theory and numerical simulations," J. Appl. Meteorol. **43**, 1513–1529 (2004).
[27]S. Luo, J. Schiffbauer, and T. Luo, "Effect of electric field non-uniformity on droplets coalescence," Phys. Chem. Chem. Phys. **18**, 29786–29796 (2016).
[28]M. Zhang, J. Li, C. Li, F. He, D. Li, K. Yu, and Y. Pan, "Investigation of the effects of parallel electric field on fog dissipation," J. Phys. D: Appl. Phys. **56**, 375204 (2023).
[29]M. H. Davis, "Two charged spherical conductors in a uniform electric field: Forces and field strength," Q. J. Mech. Appl. Math. **17**, 499–511 (1964).
[30]T. Song, X. Xing, Y. Yang, X. Li, and R. Yang, "Study on the effect of sodium polyacrylate and its compounds on artificial warm fog dissipation," AMR. **1052**, 226–230 (2014).
[31]L. P. Wang, O. Ayala, and W. W. Grabowski, "Improved formulations of the superposition method," J. Atmos. Sci. **62**, 1255–1266 (2005).
[32]M. Pinsky, A. Khain, and M. Shapiro, "Collision efficiency of drops in a wide range of Reynolds numbers: Effects of pressure on spectrum evolution," J. Atmos. Sci. **58**, 742–764 (2001).
[33]H. R. Pruppacher and J. D. Klett, *Microphysics of Clouds and Precipitation* (Kluwer Academic Publishers, Dordrecht Boston, 1997).
[34]D. C. Taflin, T. L. Ward, and E. J. Davis, "Electrified droplet fission and the Rayleigh limit," Langmuir **5**, 376–384 (1989).
[35]D. Duft, T. Achtzehn, R. Müller, B. A. Huber, and T. Leisner, "Coulomb fission: Rayleigh jets from levitated microdroplets," Nature **421**, 128 (2003).
[36]L. F. Shampine and M. W. Reichelt, "The MATLAB ODE suite," SIAM J. Sci. Comput. **18**, 1–22 (1997).